

Endocytosis in Artificial Cells

O.V. Gradov and M.A. Gradova

Vernadsky Institute of Geochemistry and Analytical Chemistry RAS, Moscow, Russia

Abstract: This paper concerns phagocytosis in artificial cells, synthesized via laser-induced self-organization. Endosomes near the artificial cell surface are investigated by grain size analysis, secondary-emission X-ray spectroscopy, scanning electron microscopy. Physical and chemical mechanisms of the phenomena observed are proposed.

Key words: Artificial cell • Endocytosis • Colloid-chemical phenomena • Granulometry

INTRODUCTION

Cytophysiological processes involving membrane structures, including endocytosis, represent a kind of colloid-chemical phenomena occurring both in organic and inorganic substrates [1]. In this regard, the mechanism of endocytosis in artificial inorganic cells can be studied as a physical-chemical process on a membrane surface.

MATERIALS AND METHODS

The samples of artificial cells, based on metacolloidal hydrogels of hydrolyzed iron salts and the polymer-immobilized dispersed semiconductors, such as GIM-AgHal (Gelatin Immobilized Matrix), were studied. The latter were synthesized according to the method [2] at the thin (0.017-0.02 mm) carrier, whose composition is given in the Table 1 below:

The structures were cultivated in a thermostatic climate chamber BINDER KBWF-240 on quartz substrates and dried in the mode of aeration before the analysis. The cultivation process was carried out in elective medium of the same elemental composition with artificial cells. Later the fragments of medium with cells were transferred to the graphite disks and subjected to carbon deposition.

The prepared samples were placed in a vacuum chamber of scanning electron microscope Oxford

Instruments and analyzed under the pressure of $12.25 \cdot 10^{-6}$ - $19.65 \cdot 10^{-6}$ Torr at a voltage of 20 kV. Detection under a high vacuum was carried out using secondary electron detector SE-1, EDX spectroscopy was performed on the detector INCA. Visualization of the elemental composition gradient was produced by the reflected electrons diffraction analyzer QBSD. A visual search and photographing of cells, carrying out their trophic function, was held in the artificial cells cultures, placed in a vacuum chamber, with the positional manipulator.

A number of artificial cells, immobilized in GIM-AgHal at the meniscus of the media, was subjected to the dehydration of plasma and dissected on microtome/cryostat. Using the method of freeze-fracture allows to record specific episodes of the artificial cells functioning in a stage, in which they were before the cryogenic treatment. This processing technology deliberately reduces the number of potential ultramicroscopic artifacts. The electron micrographs, obtained in this way, were used for grading study, as the stability of experimental conditions allowed to rank grading data for the characteristic diameter. Grain size measurements were carried out using hardware and software MEKOS in relative units, since calibration at each new level takes time, incompatible with the preservation of cells. Direct measurements of dispersion were made only *in vitro* for granules, extracted from artificial cells.

Table 1: Atomic composition of GIM-AgHal precursor.

matrix component	H	C	N	O	S	I	Br	Ag
$n, \cdot 10^{22}$ nuclei/cm ³	3.148	1.412	0.396	0.956	0.004	0.002	1.031	1.036

Model experiments with the introduction of ciliates *Paramecium caudatum* into the diluted medium were carried out for fairly large cells (> 100 microns). Slowing of paramecia's locomotor activity in a viscous medium allows one to observe the process of phagocytosis of simplest by low active artificial s phero-plasts *in vitro*. Digital microscopy images obtained in this way have been processed by Laplace transform to visualize endogenous structures, which were expected to appear in the artificial cells in response to alimentary stimulus. For stop-motion images of this process automated counting of local maxima in the parametric space, corresponding to the granular phase, was carried out.

RESULTS

From the experiment it was found that various forms of cells possess different types of phagocytosis. Artificial cells cultivated on metacolloidal gel, characterized by a strong differentiation of the surface structure with the formation of protrusions and folds such as pseudopodia. The latter are required for serving food to the oral opening (cytostome) and have sufficient energy to commit and handover of a particle through a chain of pseudopodia. Fig.1 shows an example of the "relay" on the artificial cell surface. In the foreground there are pseudopodia of capture zone, which participate in the primary fixation of aggregated microparticles from the elective medium. Then the particles are transferred by outgrowths of the second row and beyond and as seen from the illustrations, the transfer process is anticlinal. It means that first pseudopodia become in contact with each other during the particle transfer and then one of them deviates in the opposite direction, so the particle is transferred to another outgrowth. At the transfer moment, occurring almost simultaneously with the adoption of a new particle at the vacant pseudopodia, each of the pseudopodia is in one of two discrete states – in contact with the previous or the next one in the chain.

After the conveyor transfer along the chain, a particle or aggregation of particles from the extracellular medium falls into the perforation of the cell membrane and is no longer visualized by scanning electron microscopy. Fig. 2 shows this structure in the process of exogenous particles aggregate fixation. One can observe that fixing the particle is carried out by centrally-directed contraction of the elements of the cell surface, in contrast to the process of passive filtration endocytosis.

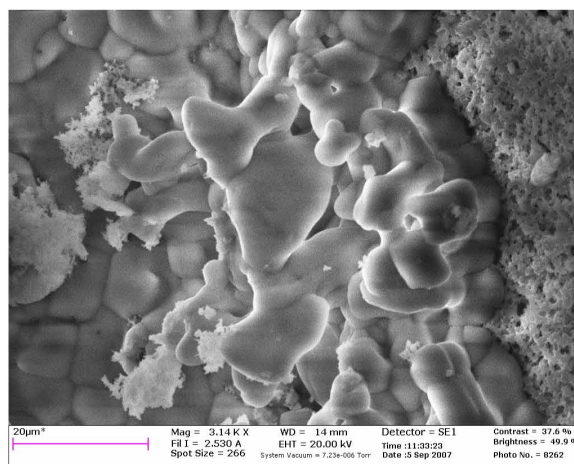


Fig. 1: A particle transfer by pseudopodia.

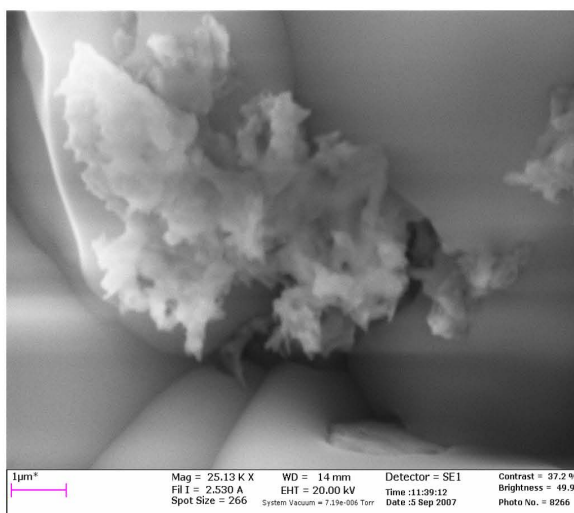


Fig. 2: The capture of particles by an pseudopodia artificial cell's "cytostome".

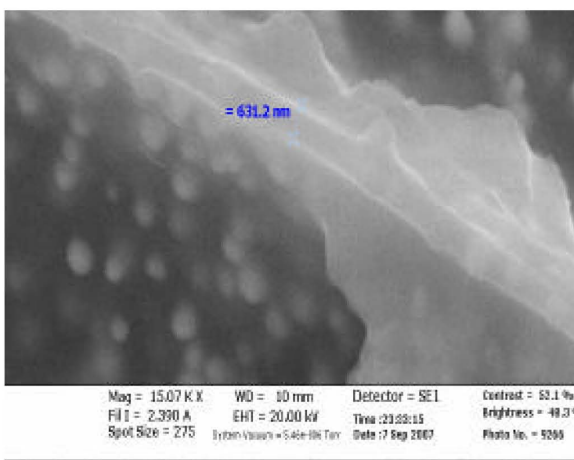


Fig. 3: Vesicular transfer through inorganic Plasmalemma via Invagination

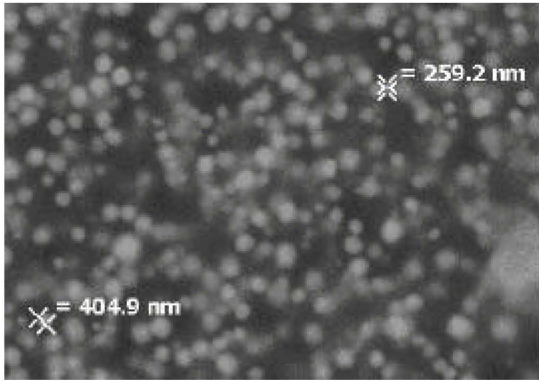


Fig. 4: Heterodispersity of inorganic phagosomes

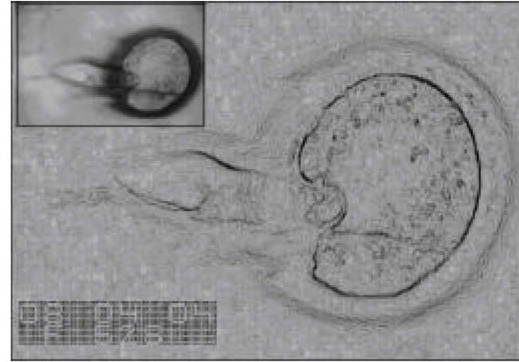


Fig. 6: Phagocytosis of Ciliata by an inorganic cell. Laplace transform.

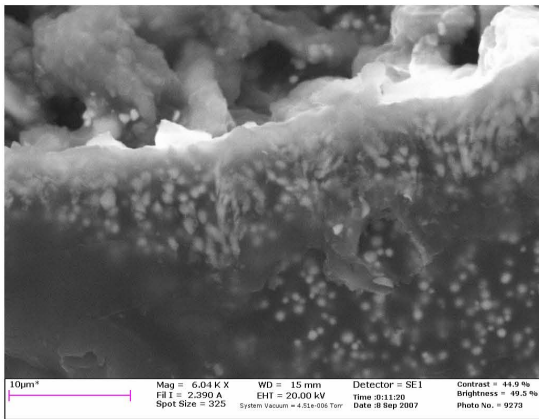


Fig. 5: Deformation of particles, passing through inorganic membrane

Unlike the cell models, synthesized and cultivated on ferriferous colloids, artificial cells, cultivated in polymer immobilization of the dispersed phase, form membrane layers with gelatin matrix. In this case, their visualization outside the polymer matrix after curing the layer becomes impossible because of the structure formation via conjugation of the dispersed precursor and the polymer gel.

Mechanism of phagocytosis in these cells differs from that described above. Endocytosis of dispersed phase particles is carried out through the invagination and phagosome formation when passing through the cell membrane. In fact, the encapsulation process is nothing

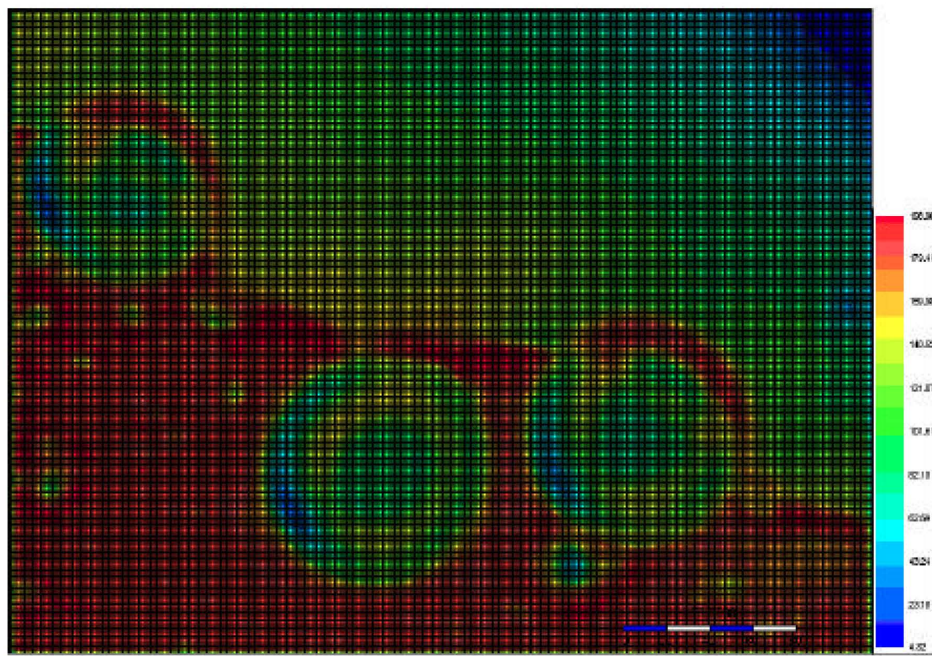


Fig. 7: Visco-elastic properties of artificial cells. The boundary layer formation on the surface outside the cultivation medium. Optical reconstruction.

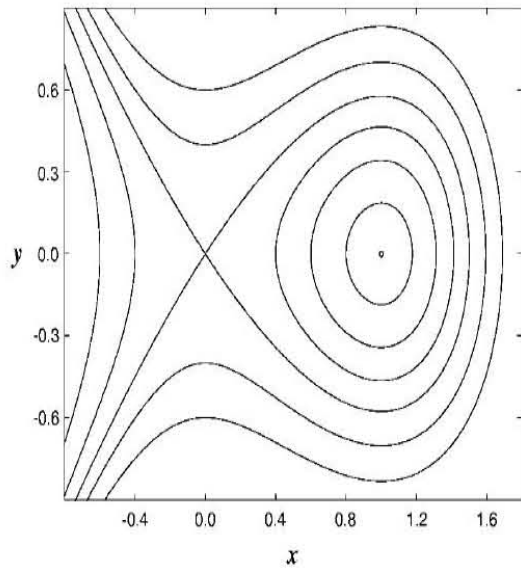


Fig. 8: Phase plane of the system at $p_1 = -1, p_2 = 1, p_3 = 0, p_4 = 0, p_5 = 0, p_6 = 2$.

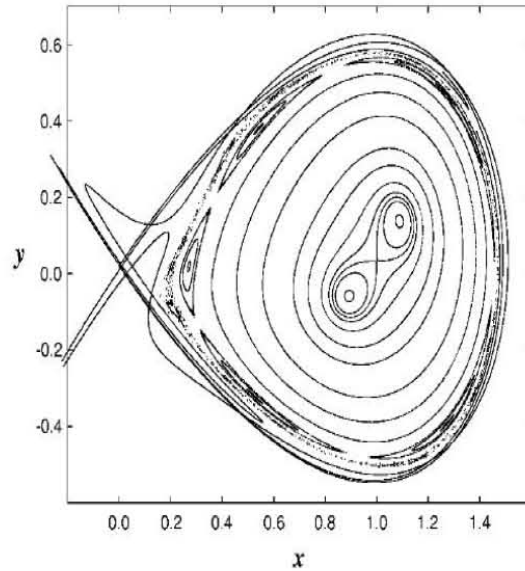


Fig. 9: The structure of system resonances at $p_1 = 1, p_2 = -1, p_3 = 0, p_4 = 0, p_5 = -0.05, p_6 = 2$.

Table 2: Grain-size measurements

D	32	34	36	38	40	46	48	52	58	60	68	$\sum_{particles}$
n	5	4	3	3	2	2	1	1	1	1	1	24

like polymer immobilization of incorporated particles in a membrane macromolecular substance. Fig. 3 shows electron micrograph of an artificial cell surface cut, obtained by the method above. At the micropreparation one can observe invaginations on the cell membrane surface from the inside. Some invaginations are in a state of detachment from the surface of the polymer layer on the stage of phagosomes. Granulometry of the endosomes indicates a high dispersion of particle sizes formed in the process of phagocytosis, as can be seen from Fig. 4. That micrograph shows two characteristic averaged over the sample values of the endosomes' diameter - 259.2 nm and 404.9 nm. However, in various cell cultures typical values of the size of endosomes vary considerably (in correlations with the size of incorporated particles).

In order to estimate the range of variations one can consider relative diameter measurements in standard units on the dispersion or r.m.s. (mean squared) granularity of the recording medium. Typically, the diameters of endosomes lie in the range of $30k < D < 70k$, where k - coefficient of proportionality, D - diameter of endosomes in relative units. The Table 2 below shows the distribution of endosome sizes in a sample of a grain-size measurement carried out near the surface of an artificial cell. From these data it follows that the number of particles n decreases with the increase of their size. Thus, the

artificial cell membrane acts as a filter for large particles.

It was found that large particles passing through the filter undergo deformations and penetrate into the cells in the ellipsoidal state. This provides penetration through the membrane into the cell only for mechanically-labile immobilized particles, because their visco-elastic properties are favorable for plastic deformation. Fig. 5 shows electron micrograph illustrating the deformation process at the stage of transformation of invaginations into phagosomes, which is localized in the cortical layer of cytoplasm beneath the artificial cell surface. A similar process seems to take place during phagocytosis of large structures.

Fig. 6 illustrates an experiment on the introduction of a ciliate *Paramecium caudatum* into a biomimetic system based on polymer film immobilized metal halides. Similar phenomena was described in [3], where vesicular cell models based on hydrophilic block copolymers "encapsulate" bacterial cells and interact with them by means of signaling molecules (saccharides). From the micrographs processed by Laplace transform it is clear that endocytosis takes place, accompanied by deformation of the ciliate from the front. At the same time elements of granular-fibrillar ultrastructure, associated with the surface of incorporated object, appear in the artificial cell cytoplasm.

Due to the rigidity of the membrane, distorting during phagocytosis in this case is less significant than at Fig. 5. This is due to the formation of a layer of high surface tension (according to hydrodynamics - the boundary layer of changed microviscosity) on the artificial cell surface. This layer, which is the basis of hydrodynamic and mechanochemical adaptability of artificial cells in a turgor state, is visualized on a map below (Fig. 7). At some sites of plasma membrane located in the liquid phase out of the cultivation medium, a formation of a layer with corresponding surface tension takes place, whereas at sites located directly in the air "above the waterline", osmotic resistance hinders to a minimum.

Similar changes associated with hydrophilic or hydrophobic and osmotic properties of artificial cells in relation to the medium and biological object, subjected to endocytosis, apparently underlie the interaction of artificial cells with Ciliata. Surface-activity of some inorganic components of plasmalemma and cortical layer are expected to be very important in this process. They can probably work as detergents, decomposing an organic substrate introduced into an artificial cell (elements of the granular ultrastructure associate with the surface of a biological object and represent bioinorganic surfactant micelles).

Mathematical Description: As revealed by the simulation, the formation of invaginations can be fairly described by a system of differential equations with a quadratic nonlinearity:

$$\begin{cases} \frac{dx}{dt} = y \\ \frac{dy}{dt} = -p_1x - p_2x^2 + (p_3 + p_4x^2)y + p_5 \sin(p_6t) \end{cases}$$

Phase plane of the system at $p_1 = -1$, $p_2 = 1$, $p_3 = 0$, $p_4 = 0$, $p_5 = 0$, $p_6 = 2$ is shown in Fig.8. The structures of system resonances in a particular case allow both formation of parietal peripheral structures (crowding), corresponding to the extrema of visco-elastic properties that are shown in Fig.7 and the possibility of location of more than one particle in invagination. An example of system resonances for $p_1 = 1$, $p_2 = -1$, $p_3 = 0$, $p_4 = 0$, $p_5 = -0.05$, $p_6 = 2$ is shown in Fig. 9.

CONCLUSIONS

Phagocytosis in artificial cells is a kind of surface phenomena and depends on the surface tension of the participating phases. Phagocytosis occurs when the surface tension between the particle and medium $W1 > W3 + W2 \cos \alpha$, where $W1$ - the surface tension between the particle and medium, $W3$ - the surface tension between the particle and the phagocyte, α - the angle between them, $W2$ - surface tension between the cell-phagocyte and the medium. The equilibrium at the point of contact is established when $W1 = W3 + W2 \cos \alpha$. A similar surface mechanism underlies a number of phenomena in synthetic cells, including cell division and cytokinesis. A mathematical model of artificial cell division also contains the conditions of separation in the form of a hyperbolic point in the phase plane and the particle-size contours of the separating plot in the form of phase trajectories of the neighborhood of an elliptic point [4]. This indicates that certain cellular processes involving the cleavage of cytoplasm or extracellular medium fragments through the membranes can be modeled using non-lipid substrates with distinct surface properties.

More complex phagocytosis mechanisms, characterized by anticyclinal traffic of particles entrained by pseudopodia to the peristome, include mechanochemical processes of unexplained origin, other than the surface tension [5]. In this regard, one can speak about the active transmembrane transport of dispersed particles in artificial cells.

REFERENCES

1. Bladergroen, W., 1949. *Physikalische Chemie in Medizin und Biologie*. Basel, pp: 675.
2. Gradov, O.V., M.A. Gradova, Rybakov S. Yu and Seo Jae Choon, 2010. *Inorganic Biomimetics for Clinical Hematology*. *Medic. Health Sci. J.*, pp: 3.
3. Pasparakis, G. And C. Alexander, 2008. *Sweet Talking Double Hydrophilic Block Copolymer Vesicles*. *Angew. Chem. Int. Ed.*, 47(26): 4847-4850.
4. Bolhovitinov, A.S., A.G. Verhovcev and O.V. Gradov, 2010. *Modeling of Artificial Cell Reproduction*. *Mat. Morph.*, 9(1): 32, [in Russian].
5. Evans, E. And R. Skalak, 1980. *Mechanics and Thermodynamics of Biomembrans*. Boca Raton, Florida, CRC Press, pp: 254.